



HAL
open science

On the possibility to simulate the operation of a SI engine using alternative gaseous fuels

Andrei Laurentiu Niculae, Lucian Miron, Radu Chiriac

► To cite this version:

Andrei Laurentiu Niculae, Lucian Miron, Radu Chiriac. On the possibility to simulate the operation of a SI engine using alternative gaseous fuels. *Tmrees, EURACA*, Sep 2019, Athènes, Greece. pp.167 - 176, 10.1016/j.egy.2019.10.035 . hal-03723936

HAL Id: hal-03723936

<https://cnam.hal.science/hal-03723936>

Submitted on 15 Jul 2022

HAL is a multi-disciplinary open access archive for the deposit and dissemination of scientific research documents, whether they are published or not. The documents may come from teaching and research institutions in France or abroad, or from public or private research centers.

L'archive ouverte pluridisciplinaire **HAL**, est destinée au dépôt et à la diffusion de documents scientifiques de niveau recherche, publiés ou non, émanant des établissements d'enseignement et de recherche français ou étrangers, des laboratoires publics ou privés.



Tmrees, EURACA, 04 to 06 September 2019, Athens, Greece

On the possibility to simulate the operation of a SI engine using alternative gaseous fuels

Andrei Laurentiu Niculae^{a,*}, Lucian Miron^a, Radu Chiriac^{a,b}

^a Faculty of Mechanical Engineering and Mechatronics, University Politehnica of Bucharest, 060042, Romania

^b EA7341 CMGPCE of Conservatoire National des Arts et Metiers, Paris, France

Received 20 September 2019; accepted 28 October 2019

Available online 13 November 2019

Abstract

A thermodynamic combustion model developed in AVL BOOST software was used in order to evaluate the pollutant emissions, performance and efficiency parameters of a spark ignition engine Renault K7M-710 fueled with compressed natural gas, hydrogen and blends of compressed natural gas and hydrogen (hythane). Multiple research studies have concluded that for the near future hythane could be the most promising alternative fuel because it has the advantages of both its components. In our previous work the model was validated for the performance and efficiency parameters by comparison of simulation results with experimental data acquired when the engine was fueled with gasoline. In this work the model was improved and can predict the values of pollutant emissions when the engine is running with the studied alternative fuels. As the percentage of hydrogen in hythane is increased, the power of the engine rises, the brake specific fuel consumption, carbon dioxide, carbon monoxide and total unburned hydrocarbon emissions decrease while nitrogen oxides increase. The values of peak fire pressure, maximum pressure derivative and peak fire temperature in cycle are higher, leading to an increased probability of knock occurrence. To avoid this phenomenon an optimum correlation between the natural gas-hydrogen blend, the air-fuel ratio, the spark advance and the engine operating condition needs to be found.

© 2019 Published by Elsevier Ltd. This is an open access article under the CC BY-NC-ND license (<http://creativecommons.org/licenses/by-nc-nd/4.0/>).

Peer-review under responsibility of the scientific committee of the TMREES, EURACA, 2019.

Keywords: Spark ignition engine; Hydrogen; Hythane; Emissions

1. Introduction

Because of depleting fossil fuel resources, alternatives to petroleum derived fuels for the internal combustion engines need to be found. Compressed natural gas (CNG) can be such an alternative fuel because is much more abundant than petroleum. It has a high H/C ratio and a high research octane number, leading to cleaner exhaust gasses than those produced by classical fuels combustion. It also has high anti-knocking proprieties but lower flame speed and shorter flammability range [1]. Hydrogen is a possible solution to overcome some of the issues faced by natural gas usage but with some limitations in terms of low storage density and current undeveloped infrastructure

* Corresponding author.

E-mail address: andrei.niculae@upb.ro (A.L. Niculae).

that does not support hydrogen as a wide-spread fuel [2]. The mixtures of hydrogen and CNG exhibits the improved properties of hydrogen as well as those of CNG. This new blend of fuel known as hythane, or HCNG, has the potential of creating a basic infrastructure for the use of hydrogen in the future.

A new combustion concept, as lean burn, is generally accepted as an effective method to simultaneously improve CNG fueled engine thermal efficiency (by increasing the heat capacity of the air-fuel mixture) and decrease exhaust emissions. As the engine runs close to the lean limit, problems such as misfiring, slower flame propagation speed and increased cycle-by-cycle variation may occur. Hydrogen addition is believed to be an ideal approach to tackle these problems [3]. By mixing the CNG with hydrogen, the mixture exhibits the advantages of hydrogen like a fast flame propagation speed, low ignition energy, and wide flammability range. However, there are limitations in using hydrogen in an internal combustion engine because the adiabatic flame temperature of hydrogen is too high, and the calorific value per unit volume of hydrogen is too low [4]. Higher NO_x emissions are obtained and a decrease of power density. Knock phenomenon may occur when the hydrogen percentage is too high. As methane percentage increases, CO₂ and HC emissions rise, and the flammability limit is shortened. Nevertheless, knock events can be reduced or even eliminated because of the good knock resistant properties of CNG [5]. These represent the reasons that an optimum hydrogen–methane blend of hythane needs to be determined.

A method that involves a low financial effort is to determine the performance parameters and the pollutant emissions of the engine when using these alternative fuels by thermodynamic simulation models (zero-dimensional models). The first law of thermodynamics provides the key equation in the incremental procedure used in these models [6].

The Wiebe function is commonly used to estimate the heat release characteristic due to its simplicity and versatility demonstrated by its forms and numerous applications. It is commonly used in internal combustion engine research as a singular, double or multiple function [7]. In Yildiz and Çeper [8] the authors present predictive simulations done by a zero-dimensional (Zero-D) single zone engine model of a SI engine fueled by methane and methane–hydrogen blends. Single and double Wiebe functions are used to model the combustion process. The results show better accuracy for the simulations performed with the double Wiebe function.

In paper [9] a Zero-D two-zone predictive model was employed to examine the effects of combustion phasing, combustion duration and cyclic variations on SI engine thermal efficiency. The authors concluded that the best efficiency will be reached when peak combustion rate occurs at about 9 °CA after TDC. Combustion phasing that deviates from this optimized value would decrease thermal efficiency. In Aliramezani et al. [10] a thermodynamic model considering flame propagation was used to predict SI engine characteristics for hydrogen–methane blends with partially charge stratification approach (direct injection of pure fuel or fuel-air mixture). The model was validated with experimental data for the natural gas at lean condition and generalized to predict the performance of the engine for a variety of hydrogen contents in hythane blends.

The authors of work [11] proposed an extended Zero-D model capable of simulating multi-fuel internal combustion engines, which takes in account the calculation of the thermodynamic properties of multiple fuel mixtures and their combustion products. Subsequently, the extended model was used to investigate the interchangeability between gaseous fuels with same Wobbe Index and the influence of inert gases (CO₂ and N₂) addition on the engine knocking resistance.

In Mariani et al. [12] a numerically simulated engine model has been developed to predict fuel consumption and NO_x emissions of a spark ignition engine fueled with hythane blends over the New European Driving Cycle. The results display the impact of the increased fuel burn rate on engine brake efficiency, fuel consumption and NO_x emissions due to hydrogen addition. HCNG blends improved engine brake efficiency, in particular at low loads and for the highest hydrogen content. These effects produced a reduction in fuel consumption. NO_x emissions increased due to higher in cylinder temperatures compared to those attained with natural gas.

2. Experimental setup

The test-cell where experiments were performed is comprised of a control room and an engine test bench (Fig. 1). The engine under test was a passenger car spark ignited (SI) Dacia Logan 1.6 K7M-710 with the technical specification presented in Table 1.

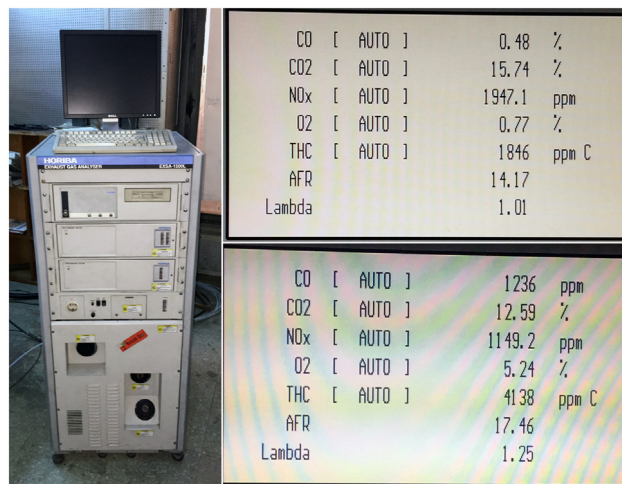
Several determinations were made at a constant speed of 2000 rpm and 2 bar brake mean effective pressure (constant load). The engine was tested in a spark timing characteristic looking for the optimum spark advance for two air-fuel ratios (AFR), respectively stoichiometric mixture $\lambda = 1$ and lean mixture $\lambda = 1.25$.

Table 1. Technical specifications of Dacia Logan engine type Renault K7M-710.

| Power | Torque | Cylinder bore | Piston stroke | Compression ratio | Valves per cylinder | Fueling system |
|----------------|-----------------|---------------|---------------|-------------------|---------------------|-----------------------|
| 64 kW/5500 rpm | 128 Nm/3000 rpm | 79.5 mm | 80.5 mm | 9.5 | 2 | Multi-point injection |

**Fig. 1.** The engine test cell with the control room and the test bench.

The ECU reference calibration maps for spark timings and for injection durations were modified using ETAS INCA v.7.2.1 software tool. For each determination, global parameters were measured using the Froude Consine Texcel V6 software. The values of pollutant emissions were measured with HORIBA EXSA-1500L gas analyzer, designed for automotive engines (Fig. 2). The AVL Indicom software was used for the pressure traces registration over 500 consecutive cycles, the mean pressure diagram and the main events specific for combustion characteristics as 5%, 10%, 50% and 90% of the heat release were also determined from the pressure diagram.

**Fig. 2.** HORIBA EXSA-1500L gas analyzer and values for pollutant emissions measured at two different conditions.

3. Simulation modeling

The AVL BOOST software was used to create a model for the K7M-710 engine. The model is made up of system boundaries (SB), pipes, air cleaner (CL), throttle (TH), injectors (I), cylinders (C), catalyst (CAT) and plenums (PL). Fig. 3 shows the symbolic model of the engine.

In this simulation tool a set of equations are used to model the engine operation. The set of conservation equations to describe a one-dimensional pipe flow is given by the well-known ‘Euler Equation System’. For modeling the combustion process, the ‘Vibe 2-Zone’ combustion model was used. The nitrogen oxides (NO_x) formation model implemented in AVL BOOST takes into account the reactions based on the well-known Zeldovich mechanism.

The carbon monoxide (CO) formation model takes into account the reactions for the oxidation of wet CO.

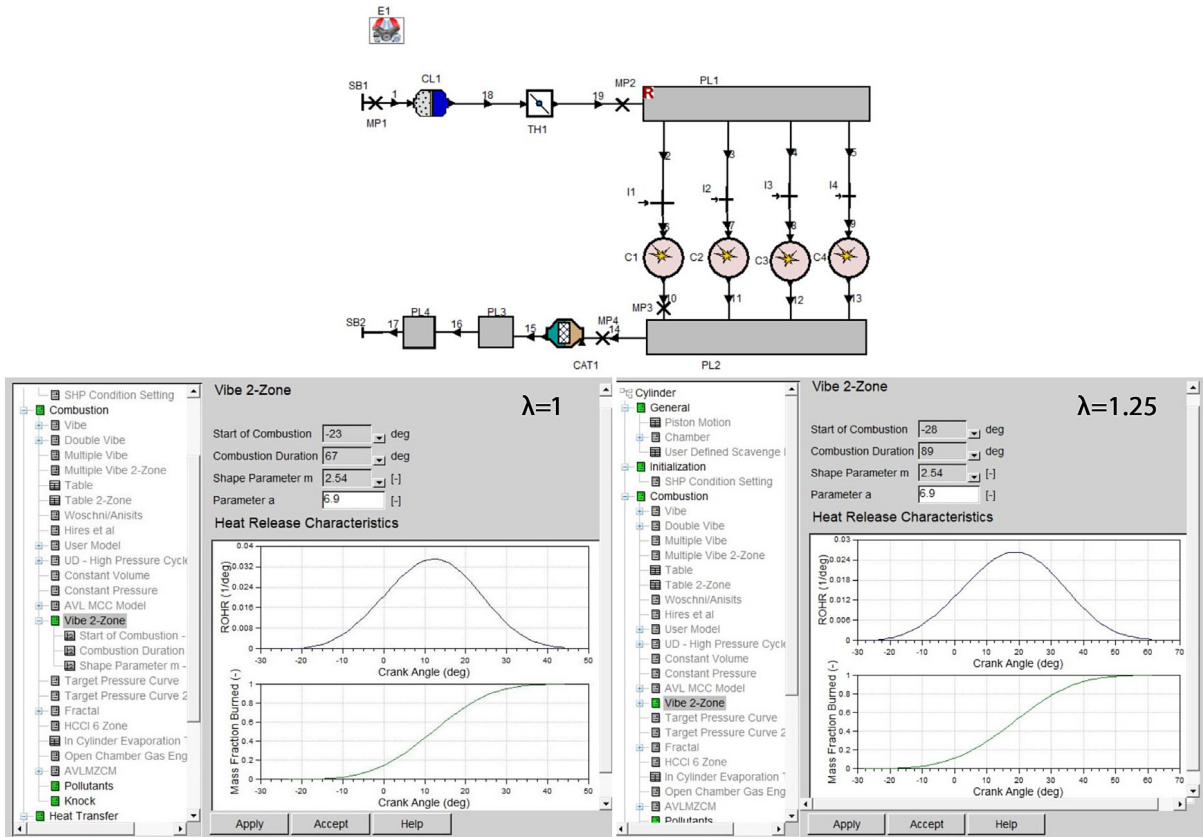


Fig. 3. K7M-710 engine model and ‘Vibe 2-Zone’ input data for the optimal spark timings.

The unburned hydrocarbons (HC) formation model considers the crevice mechanism, HC absorption/desorption mechanism, partial burn effects and the HC post oxidation. Another significant source of hydrocarbon is the presence of lubricating oil in the fuel or on the walls of the combustion chamber. Finally, all hydrocarbons released into the burned gases undergo a complex mechanism of oxidation due to the existing high temperature in the chamber. AVL BOOST use an Arrhenius equation which takes into account the slow HC post-oxidation [13].

4. Results and discussions

The performance, efficiency parameters (effective power — EP and brake specific fuel consumption — BSFC) and the combustion durations (based on the pressure diagrams) depend on the spark timing (β_s). This is reported as a positive value relative to the top dead center (TDC end of compression stroke) position.

Fig. 4 shows the measured and calculated performance and efficiency parameters variations relative to β_s when the engine was fueled with gasoline. The engine performance and efficiency are well correlated (relative deviations for EP below 4% at $\lambda = 1$ and 5% at $\lambda = 1.25$ and for BSFC below 3% at $\lambda = 1$ and respectively 4% at $\lambda = 1.25$). The optimum spark timings in terms of EP and BSFC have been considered as being 40.12 °CA for $\lambda = 1$ and 49.12 °CA for $\lambda = 1.25$. At these timings there were registered the maximum performance and the minimum specific fuel consumption.

The combustion process has been divided into two stages:

- The initial combustion stage (from β_s until when 5% of the heat was released);
- The main combustion stage (from the moment when 5% of the heat was released until the 90% of the heat was released).

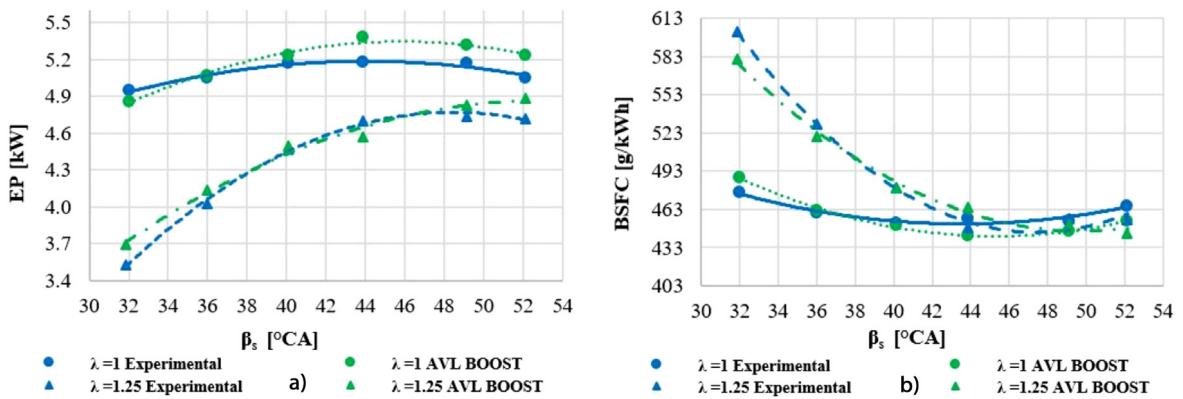


Fig. 4. Variation of effective power (a) and brake specific fuel consumption (b) versus spark timing.

The variations of these stages are shown in Fig. 5(a) for both AFR. The duration of the initial stage of the combustion process increases with 21% at $\lambda = 1$ and 30% at $\lambda = 1.25$ because the pressures and temperatures in the cylinder decrease as the spark timing is moving in advance in compression stroke in respect to TDC end of compression. The duration of the main combustion stage decreases with 19% at $\lambda = 1$ and respectively 30% at $\lambda = 1.25$ as β_s increases because the combustion takes place even further in the compression stroke where two different effects overlap (temperature increase by compression made by the piston displacement and temperature rise by the heat release by combustion). This behavior seems to be similar for both AFR but with higher values for lean mixture operation.

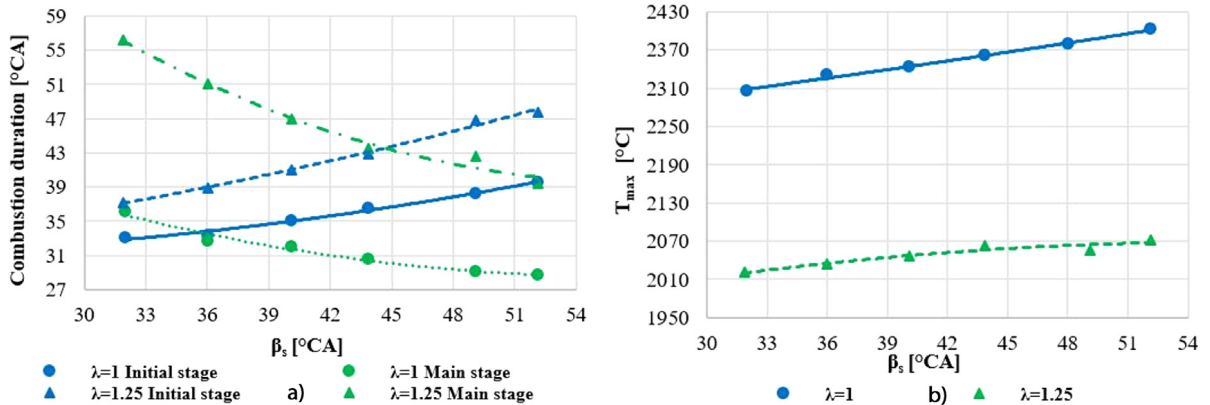


Fig. 5. Variation of the combustion stage durations (a) and in-cylinder charge peak fire temperature (b) relative to the spark timing.

The variation of the in-cylinder charge peak fire temperature is presented in Fig. 5(b) and looks much more accentuated and with higher values at the stoichiometric mixture (it rises by 4.18% at $\lambda = 1$ and only by 2.5% at $\lambda = 1.25$).

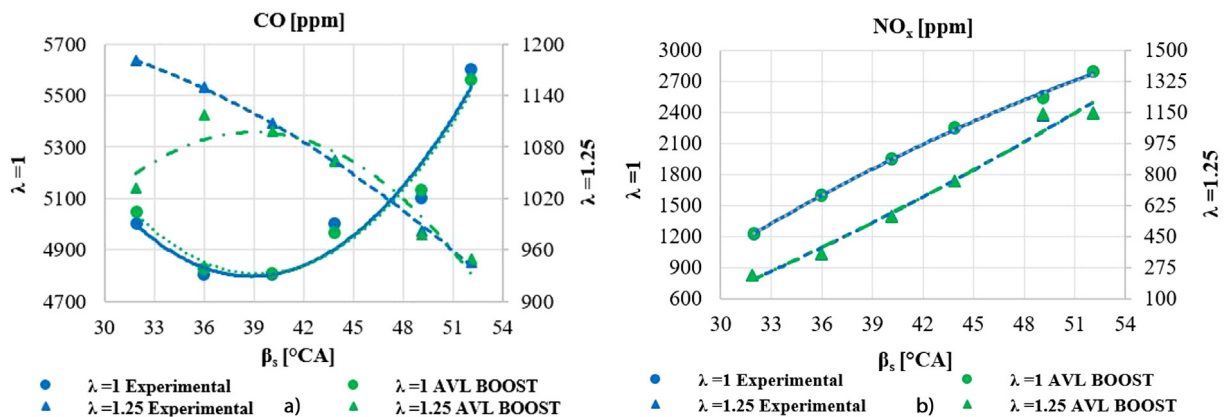
In order to compare the values of pollutant emissions calculated using the AVL BOOST software with experimentally determined emissions, different coefficients values were adopted:

- NO_x Kinetic multiplier (KM);
- NO_x Postprocessing multiplier (PM);
- CO Kinetic multiplier (KM);
- HC Postoxidation multiplier (PM);
- HC Partial burn (PB).

Table 2 shows the values adopted for the correction coefficients for these emissions in case of conventional fuel (gasoline) use.

Table 2. Values of the correction coefficients for the pollutant emissions.

| λ [-] | β_s [°CA] | NO _x | | CO | THC | | ε_{NO_x} [%] | ε_{CO} [%] | ε_{THC} [%] |
|---------------|-----------------|-----------------|--------|--------|--------|--------|--------------------------|------------------------|-------------------------|
| | | KM [-] | PM [-] | KM [-] | PM [-] | PB [-] | | | |
| 1 | 32 | 1.84 | 1.34 | 0.315 | 1 | 1500 | 0.22 | 0.88 | -0.90 |
| | 36 | 1.79 | 1.29 | 0.27 | 1 | 3300 | -0.38 | 0.49 | -0.87 |
| | 40.12 | 1.79 | 1.29 | 0.315 | 1 | 4200 | 0.29 | 0.19 | -0.29 |
| | 43.87 | 1.75 | 1.25 | 0.315 | 1 | 5800 | 0.44 | -0.69 | -0.07 |
| | 49.12 | 1.7 | 1.2 | 0.23 | 1 | 8000 | -0.72 | 0.60 | 0.01 |
| | 52.12 | 1.62 | 1.12 | 0.18 | 1 | 9200 | -0.15 | -0.76 | -0.60 |
| 1.25 | 31.87 | 2.07 | 1.57 | 0 | 1 | 33 | 0.07 | -12.59 | -0.42 |
| | 36 | 2.13 | 1.63 | 0 | 1 | 60 | 0.48 | -2.73 | 0.38 |
| | 40.12 | 2.26 | 1.76 | 0.007 | 1 | 105 | -0.53 | -0.85 | -0.75 |
| | 43.87 | 2.25 | 1.75 | 0.015 | 1 | 203 | 0.12 | -0.17 | 0.27 |
| | 49.12 | 2.6 | 2.1 | 0.019 | 1 | 305 | 0.70 | -0.42 | 0.54 |
| | 52.12 | 2.4 | 1.9 | 0.024 | 1 | 575 | -0.37 | 0.47 | 0.43 |

**Fig. 6.** Variation of the carbon monoxide (a) and nitrogen oxides (b) versus spark timing.

In next picture are presented the variation of carbon monoxide (CO) — Fig. 6(a) and nitrogen oxides (NO_x) — Fig. 6(b) versus spark timing. They show similar variation trends over the whole investigated domain with the relative errors calculated between measured and simulated values lower than 1% (except the spark timings 31.87 °CA and 36 °CA at $\lambda = 1.25$ where the relative errors are higher). In the case of stoichiometric mixture ($\lambda = 1$) the CO has an increasing variation by spark advance (β_s), while in the case of lean mixture $\lambda = 1.25$ the variation is reversed. The increase of nitrogen oxides with β_s is justified by the greater temperatures of the cylinder charge (Fig. 5(b)). The trend is fairly the same for both AFR.

Fig. 7(a) shows the variation of the total unburned hydrocarbons (THC) and Fig. 7(b) the peak fire pressure (p_{max}) variation versus spark timing. The relative errors for THC emissions are lower than 1% for both mixtures. Similar relative errors below 1% are for p_{max} at $\lambda = 1$ and below 6% at $\lambda = 1.25$ over the entire investigated domain. The duration of main combustion stage strongly affects the trend of THC emissions. The reducing of this stage causes an increase of THC emissions with β_s for both mixtures. The maximum pressure increases with spark timing because the combustion process is developed more in compression for higher spark advances.

In the work [14], a Zero-D combustion model, developed in AVL BOOST software and validated against the experimental results obtained on a spark ignition engine fueled with gasoline at stoichiometric condition was used to analyze the engine performance and emissions when pure hydrogen fuel and pure gasoline fuel operations were considered. A similar procedure was used in the current study where the model was calibrated relative to the data collected when engine was fueled with gasoline (see Figs. 4, 6 and 7) to predict further the values of pollutant emissions (CO, NO_x, THC), performance and efficiency parameters in the case of using CNG, hydrogen and hythane for the same engine operating conditions at the air-fuel ratios considered.

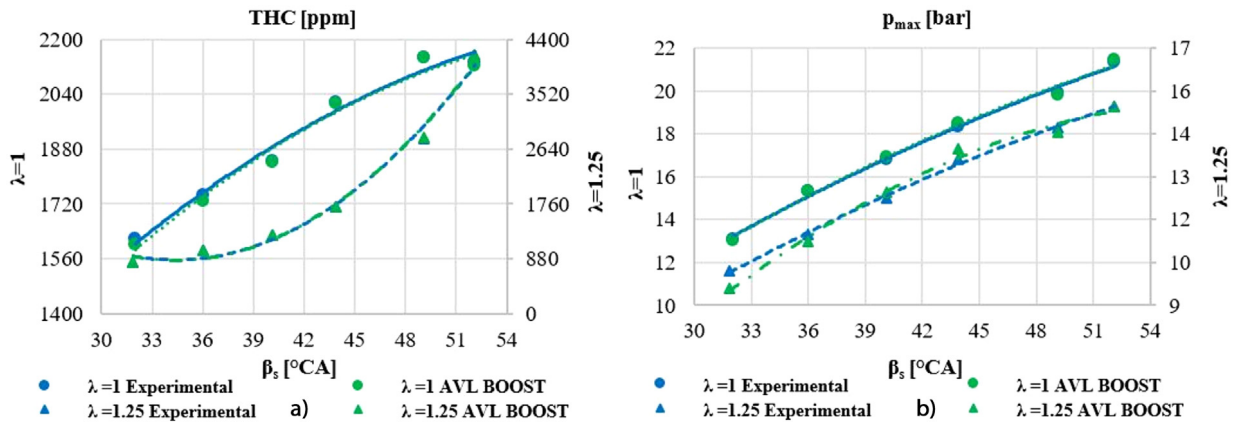


Fig. 7. Variation of the total unburned hydrocarbons (a) and peak fire pressure (b) versus spark timing.

The alternative fuels investigated with the simulation model were:

- CNG — compressed natural gas (100% methane);
- 2HCNG (2% mass fraction of hydrogen and 98% mass fraction of methane);
- 5HCNG (5% mass fraction of hydrogen and 95% mass fraction of methane);
- 20HCNG (20% mass fraction of hydrogen and 80% mass fraction of methane);
- 50HCNG (50% mass fraction of hydrogen and 50% mass fraction of methane);
- H₂ (100% hydrogen).

In order to study these mixtures ($\lambda = 1$ and $\lambda = 1.25$) the mass air flow rate was kept constant, while the fuel mass flow was changed for each of these investigated mixtures. The following simplified hypotheses have been considered:

- the start of combustion was the same regardless of the fuel used;
- the combustion duration was constant;
- the shape parameter “m” of the ‘Vibe 2-zone’ combustion model was constant;
- the values of correction coefficients for emissions adopted for gasoline were constant.

The relative deviations presented in the comments of Figs. 8–13 are calculated with respect to gasoline for the entire domain of spark timings studied.

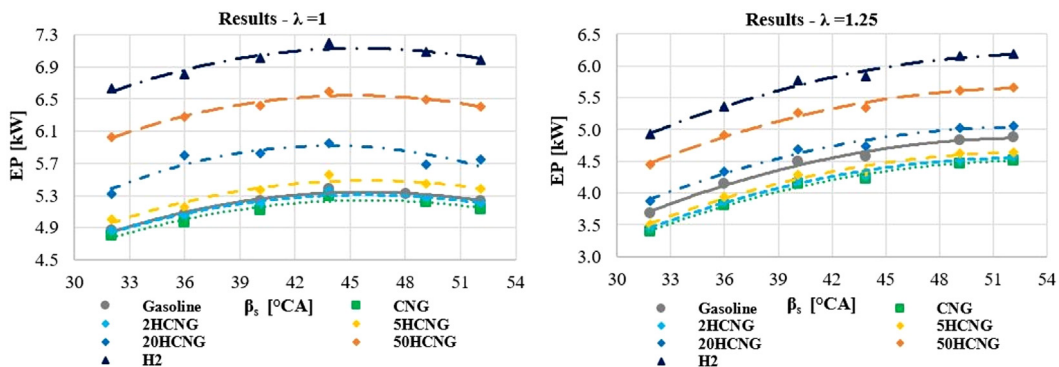


Fig. 8. Variation of the effective power versus spark timing.

In Fig. 8 is presented the variation of the effective power by spark timing. The maximum power is reached when using H₂ fuel for both mixtures (up to 34.3% more power for $\lambda = 1$ and 28.8% for $\lambda = 1.25$). The minimum power was obtained for pure CNG fuel (1.8% less power for $\lambda = 1$ and respectively 7.7% for $\lambda = 1.25$) while the addition of hydrogen to methane increases the EP of the engine.

In Fig. 9 is presented the variation of the brake specific fuel consumption relative to the spark timing. The minimum value is obtained when pure hydrogen fuel was considered (68.7% less for $\lambda = 1$ and 67.5% for $\lambda = 1.25$). The maximum BSFC was reached for the original gasoline fuel, followed by CNG with a reduction of 14.8% for $\lambda = 1$ and 9.2% for $\lambda = 1.25$. The addition of hydrogen to methane decreased the BSFC.

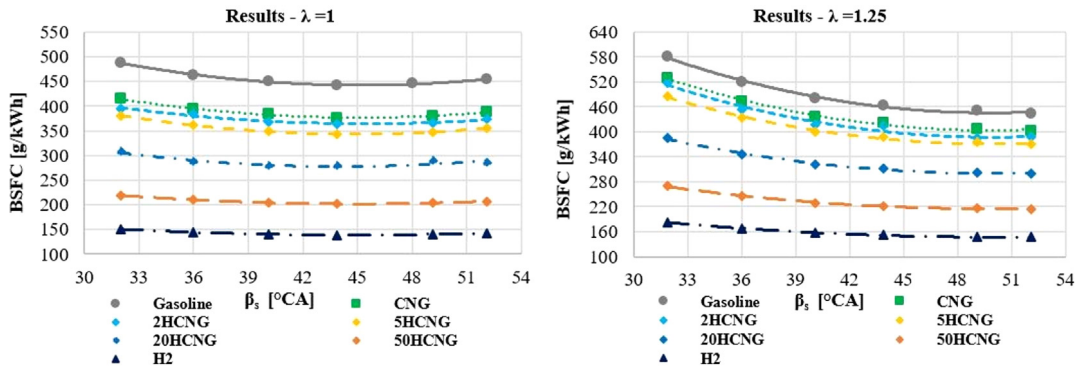


Fig. 9. Variation of the brake specific fuel consumption versus spark timing.

In Fig. 10 are presented the variations of nitrogen oxides (NO_x) relative to the spark timing for both AFR considered. The minimum values are obtained when using CNG fuel (42.6% less for $\lambda = 1$ and respectively 58.7% for $\lambda = 1.25$). The maximum values are reached when using pure hydrogen fuel (90.9% more for $\lambda = 1$ and 385.9% more for $\lambda = 1.25$). Similarly to the EP variation, by addition of hydrogen to methane the NO_x emissions increase.

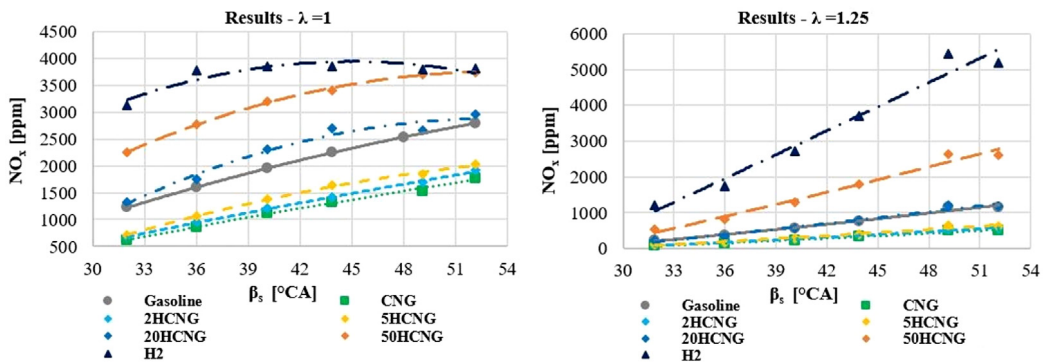


Fig. 10. Variation of the nitrogen oxides versus spark timing.

Fig. 11 shows the variation of carbon monoxide emission with respect to the spark timings in the same conditions of investigation. For pure hydrogen fueling there is no CO emission because carbon is removed from fuel. The

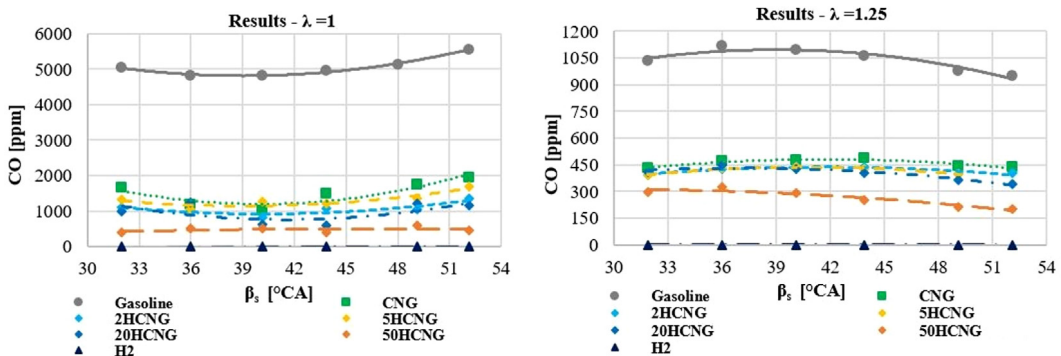


Fig. 11. Variation of the carbon monoxide versus spark timing.

maximum values for this emission are reached in case of gasoline, followed by CNG with a reduction of 70.3% for $\lambda = 1$ and respectively 55.9% for $\lambda = 1.25$. In case of hythane, the minimum values of CO emissions for $\lambda = 1$ are obtained while using 5HCNG due to the stronger dissociation effect of CO_2 caused by higher peak fire temperatures and due to the predominant reaction of hydrogen oxidation proved by higher $\text{H}_2\text{O}/\text{lower O}_2$ fractions in the exhaust gasses compared to 2HCNG which has a lower carbon content. For $\lambda = 1.25$ the minimum CO emissions are reached while using 2HCNG because these effects do not have a significant influence at lean mixtures. For 20HCNG and 50HCNG the CO emissions decrease due to the low carbon content of the fuel.

In Fig. 12 is presented the variation of total unburned hydrocarbons emission versus spark timing. The minimum values are obtained when using pure hydrogen fuel (63.8% less for $\lambda = 1$ and 64.1% for $\lambda = 1.25$). The maximum values are reached when using gasoline, followed by CNG fuel with a reduction of 17.4% for $\lambda = 1$ and 13.2% for $\lambda = 1.25$. The addition of hydrogen to methane decreases the THC emissions which are released by hythane usage.

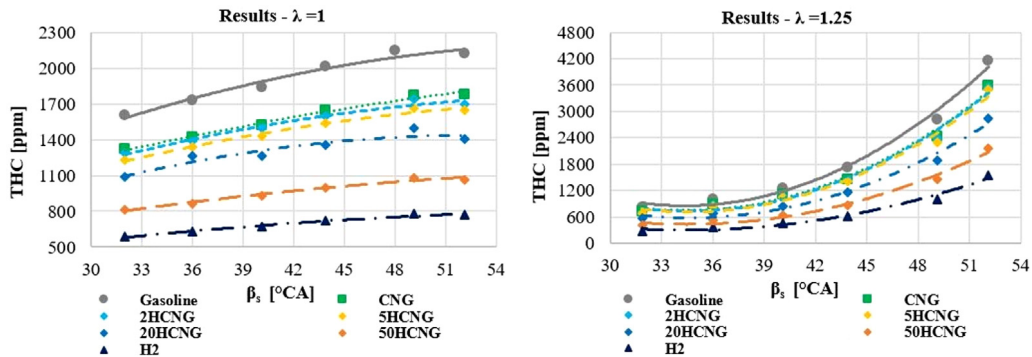


Fig. 12. Variation of the total unburned hydrocarbons versus spark timing.

Fig. 13 shows the variation of peak fire pressure (p_{\max}) in respect to the spark timing over the same investigation conditions. The minimum values of p_{\max} are obtained when using gasoline, followed by CNG with an increase of 3.3% for $\lambda = 1$ and of 2.7% for $\lambda = 1.25$. The maximum values of p_{\max} are reached when using pure hydrogen fuel with an increase of 24.4% for $\lambda = 1$ and 25.1% for $\lambda = 1.25$ relative to gasoline operation. The addition of hydrogen to methane increases the p_{\max} , reflecting the stronger influence of greater heating value of hydrogen in hythane.

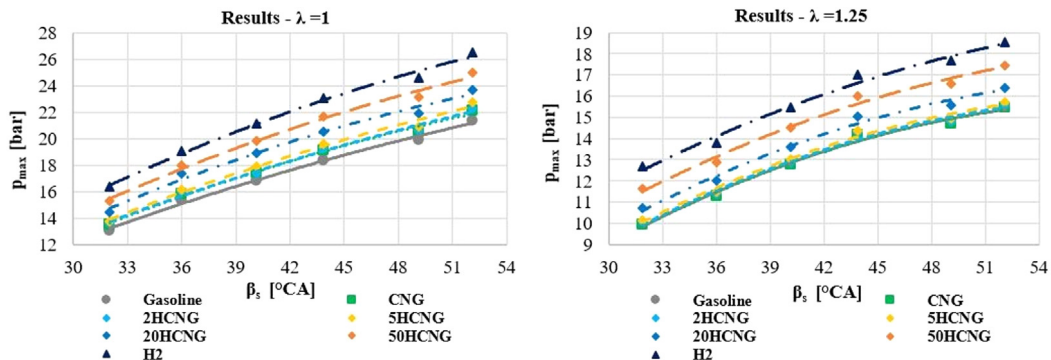


Fig. 13. Variation of the peak fire pressure versus spark timing.

5. Conclusions

The actual study aimed to show a possible solution for improving performance, efficiency and pollutant emissions of a spark ignition engine when using alternative fuels (CNG, 2HCNG, 5HCNG, 20HCNG, H_2) based on simulations developed with a Zero-D AVL BOOST combustion model. The model has been successfully calibrated for effective power, brake specific fuel consumption, peak fire pressure and pollutant emissions (NO_x , CO, THC) on gasoline usage. The results showed that the use of hythane blends increases engine performance and efficiency and

significantly reduces the CO, THC, but increases the NO_x emissions and peak fire pressures. For example, in the case of 20HCNG average values of 10.4% more power, 37.1% less brake specific fuel consumption, 80.9% less CO, 31.3% less THC, 11.1% higher NO_x and 11.3% higher peak fire pressure comparing to gasoline at $\lambda = 1$ were obtained. Higher mass fraction of hydrogen in hythane mixture accentuates these effects so an optimum hythane blend needs to be found and must be correlated with the engine global energetic formula and its application.

The research carried out illustrates that the use of thermodynamic simulation models can be an efficient method for engines development. Detailed experimental and numerical investigations are still required to validate the improved operation of the spark ignition engines with this new type of fuel.

Acknowledgment

The authors acknowledge the AVL-AST team from AVL List GmbH for the special support offered under the UPP program.

References

- [1] F. Ma, N. Naeve, M. Wang, L. Jiang, R. Chen, S. Zhao, Hydrogen-enriched compressed natural gas as a fuel for engines, in: *Natural gas*, ISBN: 978-953-307-112-1, 2010.
- [2] S.M.V. Sagar, A.K. Agarwal, Hydrogen-enriched compressed natural gas: An alternate fuel for IC engines, *Adv Intern Combust Engine Res* (2018) <http://dx.doi.org/10.5772/9852>.
- [3] P.T. Nitnaware, J.G. Suryawanshi, Effects of lean burn and stoichiometric combustion on multi-cylinder SI engine using hydrogen and CNG blends, *Iran J Sci Technol: Trans Mech Eng* 40 (2016).
- [4] G. Lim, S. Lee, C. Park, Y. Choi, C. Kim, Effect of ignition timing retard strategy on NO_x reduction in hydrogen-compressed natural gas blend engine with increased compression ratio, *Int J Hydrogen Energy* 39 (2014) 2399–2408.
- [5] F. Moreno, M. Munoz, J. Arroyo, O. Magen, C. Monne, I. Suelves, Efficiency and emissions in a vehicle spark ignition engine fueled with hydrogen and methane blends, *Int J Hydrogen Energy* 37 (2012) 11495–11503.
- [6] V. Shree, V. Ganesan, Thermodynamic modelling of combustion process in a spark ignition engine and its numerical prediction, *Combust Power Gener Transp* (2017).
- [7] J.I. Ghojel, Review of the development and applications of the wiebe function: a tribute to the contribution of Ivan Wiebe to engine research, *Int J Engine Res* 11 (2010).
- [8] M. Yildiz, B.A. Çeper, Zero-dimensional single zone engine modeling of an SI engine fuelled with methane and methane-hydrogen blend using single and double wiebe function: A comparative study, *Int J Hydrogen Energy* 42 (2017) 25756–25765.
- [9] F. Ma, Y. Wang, J. Wang, S. Ding, Y. Wang, S. Zhao, Effects of combustion phasing, combustion duration, and their cyclic variations on spark-ignition (SI) engine efficiency, *Energy Fuels* 22 (2008) 3022–3028.
- [10] M. Aliramezani, I. Chitsaz, A.A. Mozafari, Thermodynamic modeling of partially stratified charge engine characteristics for hydrogen-methane blends at ultra-lean conditions, *Int J Hydrogen Energy* 38 (2013) 10640–10647.
- [11] L. Xiang, G. Theotokatos, Y. Ding, Investigation on gaseous fuels interchangeability with an extended zero-dimensional engine model, *Energy Convers Manage* 183 (2019) 500–514.
- [12] A. Mariani, B. Morrone, A. Unich, Numerical evaluation of internal combustion spark ignition engines performance fuelled with hydrogen – natural gas blends, *Int J Hydrogen Energy* 37 (2012) 2644–2654.
- [13] AVL-BOOST Theory (2016).
- [14] Y. Karagöz, O. Balci, H. Köten, Investigation of hydrogen usage on combustion characteristics and emissions of a spark ignition engine, *Int J Hydrogen Energy* 44 (2019) 14243–14256.